PERGAMON

Vision Research 38 (1998) 2801–2816

Vision Research

# Second-order motions contribute to vection

Rick Gurnsey [a,*], David Fleet [b], Cindy Potechin [a]

[a] *Department of Psychology, Concordia University, 7141 Sherbrooke Street West, Montréal, Québec H4B 1R6, Canada*
[b] *Department of Computing and Information Science, Queen's University, Kingston, Ontario, Canada*

Received 17 January 1997; received in revised form 14 July 1997

**Abstract**

First- and second-order motions differ in their ability to induce motion aftereffects (MAEs) and the kinetic depth effect (KDE). To test whether second-order stimuli support computations relating to motion-in-depth we examined the vection illusion (illusory self motion induced by image flow) using a vection stimulus (**V**, expanding concentric rings) that depicted a linear path through a circular tunnel. The set of vection stimuli contained differing amounts of first- and second-order motion energy (ME). Subjects reported the duration of the perceived MAEs and the duration of their vection percept. In Experiment 1 both MAEs and vection durations were longest when the first-order (Fourier) components of **V** were present in the stimulus. In Experiment 2, **V** was multiplicatively combined with static noise carriers having different check sizes. The amount of first-order ME associated with **V** increases with check size. MAEs were found to increase with check size but vection durations were unaffected. In general MAEs depend on the amount of first-order ME present in the signal. Vection, on the other hand, appears to depend on a representation of image flow that combines first- and second-order ME. 

*Keywords:* Vection; Self-motion; Motion-aftereffects; Motion; Second-order motion

## 1. First-order and second-order motion mechanisms

It is well-known that all the power of a coherently translating signal lies on a plane through the origin of its 3D Fourier transform [1–3] and that motion energy (ME) mechanisms, which are selective for restricted regions in the Fourier domain, provide a useful basis for the estimation of local translatory motion [1,4]. An ME mechanism involves an initial stage of linear spatiotemporal filtering followed by a squaring nonlinearity and a local pooling of responses to encode the energy that a signal contains in a given volume in the 3D Fourier domain. The responses of a number of ME mechanisms that cover the 3D Fourier domain can be used to determine the plane that contains most of the power and thereby provide an estimate of the local image velocity. Those image motions for which ME mechanisms can provide accurate estimates of local velocity have become known as first-order motions, and the structures that encode them have become known as the first-order (Fourier) pathway.

There are many cases in which motion signals are perceived to have a definite velocity even though this velocity cannot be recovered directly from the distribution of power in the Fourier domain. Such signals are known as second-order (non-Fourier) stimuli [5,6]. Examples of second-order stimuli include the motion of contrast envelopes [7,8], texture boundaries [9–11] and motion boundaries [12]. For these stimuli the perceived velocity cannot be explained directly through the principle locations of power in the Fourier domain. Therefore, to account for the perception of second-order motions, several authors have proposed the existence of a second motion pathway which differs from the first-order pathway in that ME computations follow an initial stage of spatiotemporal filtering and a non-linear transformation of the filtered signal [13,6,5,14,10,15].

## 2. Percepts arising from first- and second-order stimuli

The distinction between first-order and second-order motions appears to be more than a formal one. Although one can readily perceive simple properties of second-order motions such as speed [16] there are dif-

* Corresponding author. Tel.: +1 514 8482243; fax: +1 514 8484545; e-mail: gurnsey@vax2.concordia.ca.

0042-6989/98/$19.00 
PII: S0042-6989(97)00456-2

ferent perceptual consequences of exposure to first-order and second-order stimuli. For example, second-order motions produce weaker motion aftereffects (MAEs) to static test stimuli than do first-order stimuli [17,18].[1] It should be noted however, that motion aftereffects to second-order stimuli do arise when the test stimulus involves dynamic noise [7]. Also, second-order motions do not permit the recovery of 3D structure from motion requiring high spatial resolution (which we refer to as the kinetic depth effect (KDE)) [19–21].[2] These results are consistent with the proposal that first-order and second-order motions are encoded by different mechanisms.

Unlike the main body of research on second-order motion which concerns detection thresholds, velocity discrimination, and MAE, Landy et al. [19] asked whether second-order motions could support the KDE. In their experiments subjects had to identify objects on the basis of their 3D structure which was conveyed by the relative image motions of limited-lifetime dots. Individual dot paths were given by first-order or second-order motions. Their results indicated that 3D structure could only be extracted from stimuli that engage first-order energy mechanisms; that is, second-order motions do not support the KDE (for a brief review see [23]). This result is related to the idea popularized by Livingstone and Hubel [24] that motion of isoluminant colour contours cannot support depth perception (cf [5,25]).

Fleet and Langley [14] argued that first-order and second-order signals may arise from distinct physical causes. From this perspective, first-order and second-order motion paths may be subject to different computational constraints, and serve different visual functions. For example, optic flow arising from the relative 3D motions of textured surfaces may be processed primarily by first-order channels. Second-order motions may be associated with transparency and occlusion [26,27]. (A similar distinction was drawn by Gurnsey and von Grünau [10].) In support of this point Fleet and Langley [28] showed that certain stereoscopically presented contrast modulations of a sinusoidal carrier grating can be perceived transparently in front of, but not behind, the carrier. When the waveforms of the grating and the contrast envelope were added rather than multiplied together, either waveform could be perceived in front or behind. To explain this they proposed that different computational constraints are used by the visual system to interpret additive transparency and multiplicative (second-order) transparency.

[1] This is a bit puzzling in view of the fact that existing models concieve the mechanisms involved in both channels to have computationally similar forms: i.e. motion energy mechanisms that differ only in the representations to which they are applied [15,10].

[2] Note that Prazdny [22] showed that structure could be recovered from second-order motion when the structures involved were simple forms.

In contrast to the view that first-order and second-order motion mechanisms subserve different visual functions Wilson et al. [15] proposed a model in which the responses of first-order and second-order channels are pooled for the purpose of computing image motion. If one views the visual system as a hierarchy then the computation of optic flow may be placed prior to the extraction of structure from motion, direction of heading and time to collision. The computation of optical flow may be seen as providing the input to these 'higher-order computations'. Can these higher-order, biologically relevant computations can be supported by second-order motions? The results of Landy et al. [19] suggest that the answer is no. Here, we address a similar question using a somewhat different paradigm. Specifically we ask whether second-order stimuli can induce the vection illusion.

## 3. Vection

Vection is a visuo-vestibular illusion in which image flow induces a perception of self-motion [29,30]. Linear vection [29] is the experience of illusory translatory motion induced by image motion. Circular vection [31] is the experience of illusory rotary motion induced by retinal image motion. With respect to the kinds of biologically relevant visual computations that can be supported by second-order motions, vection is an excellent object of study.

The perception of self-motion is a biologically relevant response that seems logically dependent on the computation of optic flow. Vection shares with the KDE the connection between image flow and depth, but the flow fields used to induce vection may be simpler. For example, one can create a vection stimulus (optic flow pattern) in which image velocity remains constant at a point. By comparison, when complex objects like those used by Landy et al. [19] move in 3D, the image velocities change significantly over time at each retinal position. In this paper we are interested in the relationship between the strength of the vection illusion and MAE induced by particular stimuli. The relative simplicity of the vection stimuli described below allows us to test both the strength of the vection illusion and MAE induced by patterns with fixed velocity at each image point.

## 4. Physiology

Single-cell recordings have shown that neurons in visual cortical areas respond to second-order motions [32–37]. Both cortical areas V1 and V2 provide input to visual area MT which appears central to the processing of visual motion. It is also believed that neurons in MT

integrate motion signals from V1 and V2, being selective for the intersection of constraints direction of motion plaids, while V1 and V2 neurons respond only to the directions of the plaid components [38,4]. The model of Wilson et al. [15] shares the assumption that 1D components are integrated at MT but assumes that an additional second-order channel (identified with V2) provides input to MT. The second-order channel output is combined with output from a first-order motion channel (identified with V1) to encode plaid direction through an elaborated vector sum process.

Recent physiological data reported by Duffy and Wurtz [39,40] suggest that cells in MSTd respond to flow fields related to egomotion, including radial expansion. Such cells could play a major role in the perception of self motion, direction of heading and the generation of the vection illusion. In physiological terms, the question addressed here is whether the neurons in V1, V2, or MT that respond to second-order motions provide input to MSTd to drive neurons tuned to radial expansion and to thereby induce vection.

## 5. The basic vection signal

Our basic vection signal is a depiction of a forward linear path through a cylindrical tunnel whose walls are 'painted' with a sinusoidal grating. The form of the perspective projection of the tunnel walls onto the image is given by Eq. (1):

$$\mathbf{V}(x, y, t) = \sin[2\pi \mathbf{c}/d + 2\pi\omega t] \quad (1)$$

where $d = (x^2 + y^2)^{-1/2}$ is distance from the centre (origin) of the image, $c/d$ is the spatial frequency of the image stimulus at $d$, $t$ indexes time, and $\omega$ is temporal frequency. The spatial frequency of $\mathbf{V}(x, y, t)$ decreases as a function of distance from the origin, $d$. Accordingly, with temporal frequency $\omega$ fixed at 3 Hz, the instantaneous velocity increases as a function of $d$.

From Eq. (1), one can derive a conventional 'first-order' vection stimulus having the form

$$\mathbf{S}_0(x, y, t) = \mu + \alpha \mathbf{V}(x, y, t) \quad (2)$$

where $\alpha$ is the amplitude of the mean-zero vection signal, and $\mu$, the mean luminance, is chosen so that $\mathbf{S}_0(x, y, t) \geq 0$. This served as our control stimulus, a static version of which is shown in the top panel of Fig. 1. The central region of the stimulus has been set to a uniform grey to hide aliasing caused by high spatial frequencies.

The middle panel of Fig. 1 shows a space-time slice of the $\mathbf{S}_0(x, y, t)$ taken through the origin, with $y = 0$. In this representation image speed and direction are given by space-time orientation with vertical representing zero speed. The insets of the middle panel show the even and odd components of a Gabor filter tuned to leftward motion. The bottom panel shows the motion energy extracted using this filter. The ME mechanism correctly responds to the local leftward motion in the signal and, as noted earlier, the response of the ME unit at a particular point in space is invariant over time.

## 6. Carrier signals and contrast envelopes

To create a larger class of vection stimuli including both first- and second-order patterns, the basic vection stimulus in Eq. (1) was used as a contrast envelope which modulated the amplitude of a carrier signal. The modulating contrast envelope has the form

$$\mathbf{M}(x, y, t) = 1.0 + \mathbf{V}(x, y, t) \quad (3)$$

Here, $\mathbf{M}(x, y, t)$ takes on values between 0 and 2.

Three different carriers were used, referred to here as the concentric, noise and radial patterns. Examples are

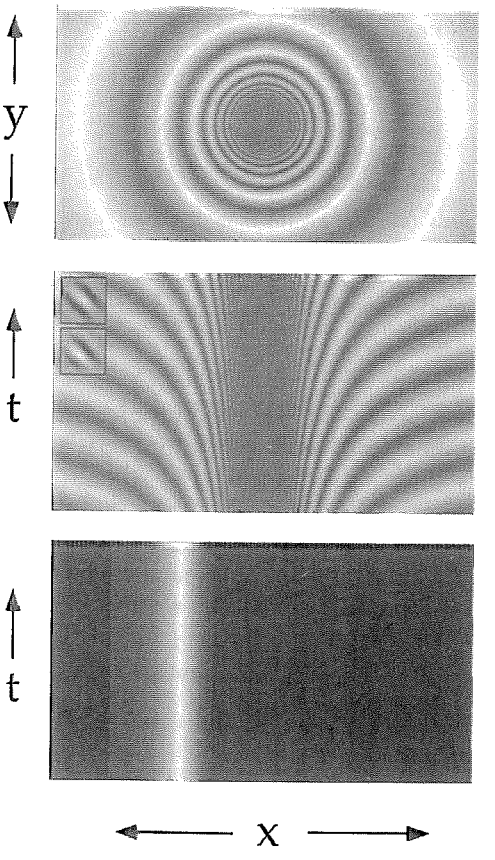


Fig. 1. Space-time analysis of the basic vection stimulus $\mathbf{S}_0(x, y, t)$ from Eq. (2). (Note, the central disk has been set to a uniform grey to obscure aliasing that occurs for very high frequencies.) The middle panel shows a space-time slice of $\mathbf{S}_0(x, y, t)$. The spatial dimension ($x$) represents a cross-section that runs through the centre of the stimulus. The insets show the odd and even components of the Gabor filter used to extract motion energy from the space- time slice. The bottom panel shows the motion energy response. Energy is clearly localized to the left of centre where the leftward motion of the stimulus matches the tuning of the Gabor filter.

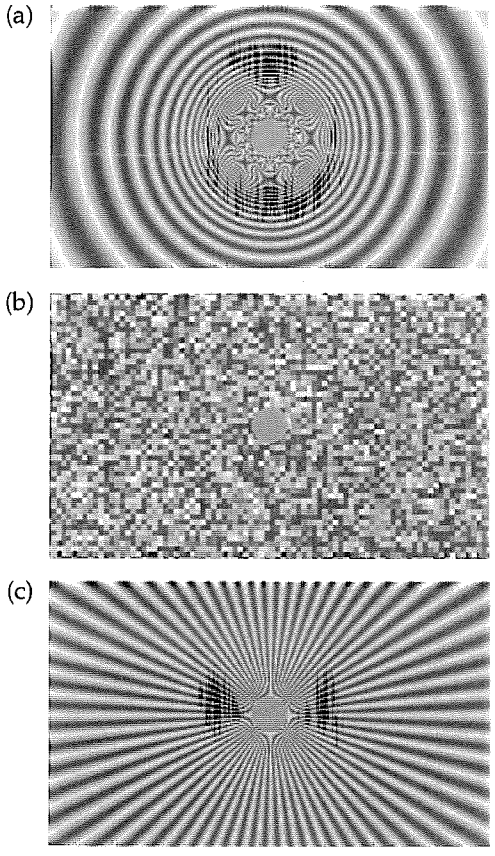


Fig. 2. Panels (a), (b) and (c) show the three static carriers. The concentric carrier (a) has exactly the same form as $\mathbf{V}(x, y, t)$ but at each eccentricity $d$, its spatial frequency, is three times that of $M$. The noise carrier (b) is quasi-random noise. The radial carrier (d) is a sinusoidal function of angle and goes through 64 cycles per 360 degrees.

shown in Fig. 2a–c. The concentric carrier (Fig. 2a) had the same form as **V** but with a spatial frequency that was three times higher. The second carrier was random noise (Fig. 2b).[3] The radial carrier (Fig. 2c) depicts a tunnel with lines of constant intensity running through the tunnel, with a sinusoidal cross-section of 64 cycles. All three carriers can be written as

$$\mathbf{C}(x, y, t) = n + \mathbf{D}(x, y, t) \tag{4}$$

where $\mathbf{D}(x, y, t)$ is one of the three carrier patterns, each of which was mean-zero with values between $-1$ and 1, and $n$ is the mean of $\mathbf{C}(x, y, t)$.

## 7. Combining the modulator and carrier

The carriers and the modulator were multiplied to yield stimuli of the form

$$\mathbf{S}(x, y, t) = \mu + \alpha\mathbf{M}(x, y, t)\mathbf{C}(x, y, t) \tag{5}$$

The constant $\mu$ was chosen so that $\mathbf{S}(x, y, t) \geq 0$, and the constant $\alpha$ was used to control the average contrast of the stimulus. If Eq. (5) is expanded using Eqs. (2) and (3), then the form of the stimuli is evident in greater detail:

$$\begin{aligned}\mathbf{S} &= \mu + \alpha[1.0 + \mathbf{V}][n + \mathbf{D}] \\ &= (\mu + \alpha n) + \alpha n\mathbf{V} + \alpha\mathbf{D} + \alpha\mathbf{VD}.\end{aligned} \tag{6}$$

In what follows we will abuse notation somewhat and drop the dependence of these terms on $x$, $y$, and $t$. Eq. (6) shows that the stimuli contain four terms, namely, a constant, a term containing the basic vection signal, a term containing the carrier pattern, and a term containing the product of the vection signal and the carrier. The explicit presence of the local first-order components of the vection signal **V** depends on the constant parameter, $n$.

In Experiment 1 each carrier signal was combined multiplicatively with the vection signal, with three values of $n$. This yields nine stimuli which are shown in Fig. 3. Note that the modulator $(1.0 + \mathbf{V})$ takes on values between 0 and 2, and the carrier **D** takes on values between $-1$ and 1. In Experiment 1 reported below, the value of $\alpha$ was set to 0.3 fL and the value of $\mu$ was set to 1.33 fL. In Experiment 2 the value of $\alpha$ was set to 0.6 fL and the value of $\mu$ was set to 2.66 fL.

## 8. The effect of varying *n*

The constant $n$ has a critical effect on the properties of the stimuli in Eq. (6). The cases of interest are those in which $n = 0$, $n = 1$ and $n = -1$. When $n = 0$ Eq. (6) reduces to

$$\mu + \alpha\mathbf{D} + \alpha\mathbf{VD}. \tag{7}$$

The vection signal, **V**, exists only in the product with **D** so that the local first-order components of **V** are not explicitly present in **S**. By comparison, when $n$ is 1 or $-1$ the vection signal **V** occurs explicitly as one of the terms in the stimulus **S**. This is evident in Eq. (6). Thus, when $n = 1$ or $-1$ there is first- and second-order information in the stimulus that is consistent with the local structure **V**.

The mean of **S** varies with $n$. For $n = -1, 0$ and 1 the mean of **S** is $\mu - \alpha$, $\mu$ and $\mu + \alpha$, respectively. The contrast of **S** also changes with $n$, although the exact nature of this change depends of how contrast is defined. Using the standard Michelson contrast

$$C = (L_{max} - L_{min})/(L_{max} + L_{min}) \tag{8}$$

where $L_{max}$ and $L_{min}$ refer to the highest and lowest pixel intensities respectively, contrast is inversely related to $n$. For $n = -1, 0$ and 1 the Michelson contrasts are

[3] The noise signal at each check was given by $\sin(u)$ where $u$ was a uniform random variable between 0 and $2\pi$. Check size was $2 \times 2$ pixels.

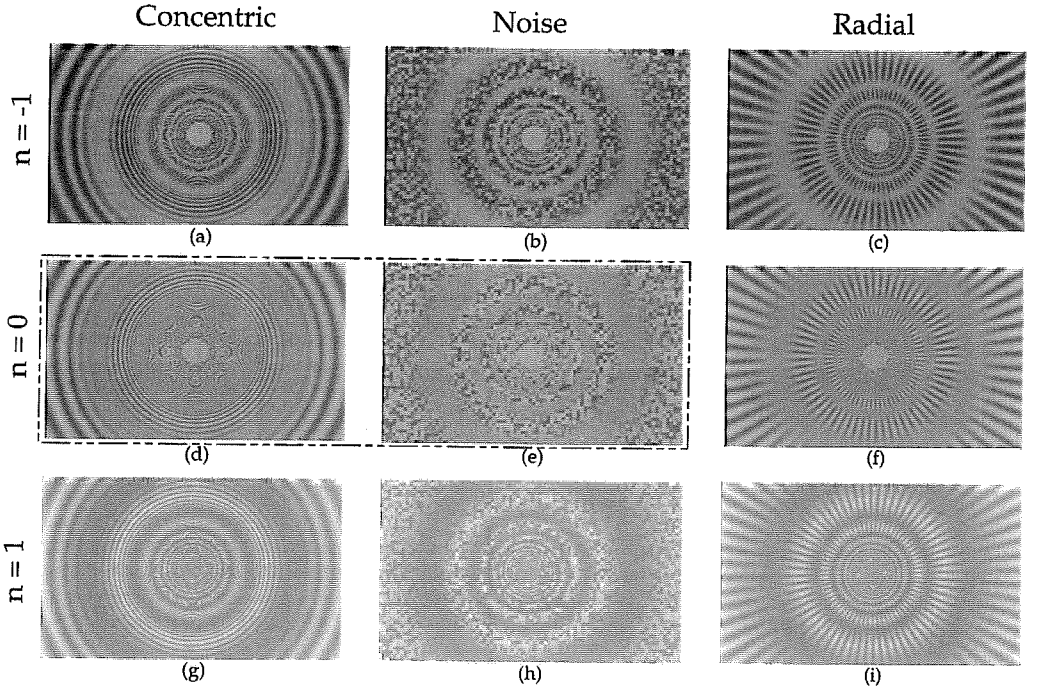


Fig. 3. Examples of the nine stimuli used in Experiment 1. $V(x, y, t)$ was combined multiplicatively with the concentric, noise and radial carriers. In panels a–c, $n = -1$, d – f, $n = 0$, and g–i, $n = 1$. Panels d and e are second-order stimuli.

0.82, 0.45 and 0.31, respectively. If contrast is defined in terms of the expected mean intensities in the peaks ($L_{max}$) and troughs ($L_{min}$) of the contrast modulations then the contrasts for $n = -1$, 0 and 1 are 0.29, 0.0 and 0.18. These contrasts now show a strong quadratic dependence on $n$ with a minimum at $n = 0$ due to the fact that the expected mean luminance is the same in the peaks and troughs of the contrast modulation. Finally, a measure of the depth of the contrast modulation given by

$$M = (C_{max} - C_{min})/(C_{max} + C_{min}) \quad (9)$$

(where $C_{max}$ and $C_{min}$ refer to the maximum and minimum contrasts in the image as defined by Eq. (8)) is not informative because $M = 1$ for all values of $n$ ($C_{min}$ is zero irrespective of $n$).

### 8.1. Concentric and noise carriers

The practical question is how variations in $n$ affect ME mechanisms in first- and second-order channels. The ME analysis described in Fig. 1 was applied to the image intensities of the contrast modulated noise carriers having $n = 0$ and 1 (Fig. 4, left columns). (Although the analysis in Fig. 4 involves Noise carriers it applies equally to Concentric carriers. The Radial carriers, however, require a slightly different treatment.) The same analysis was applied to a non-linear transformation of the luminance values. Specifically, each spatial slice in the space-time representation of the signal was convolved with a small centre-surround filter and the results were half-wave rectified. The ME mechanism was then applied to the these rectified filter responses (Fig. 4, right columns) to provide a model of a second-order channel. The effect of varying n is seen clearly in the first-order channel. Fig. 4 (left two panels) shows that for both stimuli there are energy responses on both sides of the vertical midline. This contrasts with Fig. 1 in which ME was completely localized to the left of the vertical midline. However, when $n = 1$ the responses are asymmetrical. The responses on the left side are much larger, where the local translation of V is leftward. Because of the contradictory information introduced by the carriers, there is still a weak energy response on the right side. When $n = 0$ the energy responses are far weaker than when $n = 1$, and the responses on the left and right have similar magnitudes.

For the second-order channel ME responses are asymmetrical for both $n = 0$ and $n = 1$. The second-order channel responds to the drift of the contrast modulation which is present whether or not the local first-order components of V are present. For this particular model of a second-order channel, second-order ME responses are very similar for both values of $n$ and are overall somewhat lower than the responses of the first-order channel. These examples indicate that setting $n$ to 0 eliminates a substantial amount of first-order ME from the signal (Fig. 4, second column) while leaving the second-order channel relatively unaffected (assuming that the second-order channel operates more or less as described above).

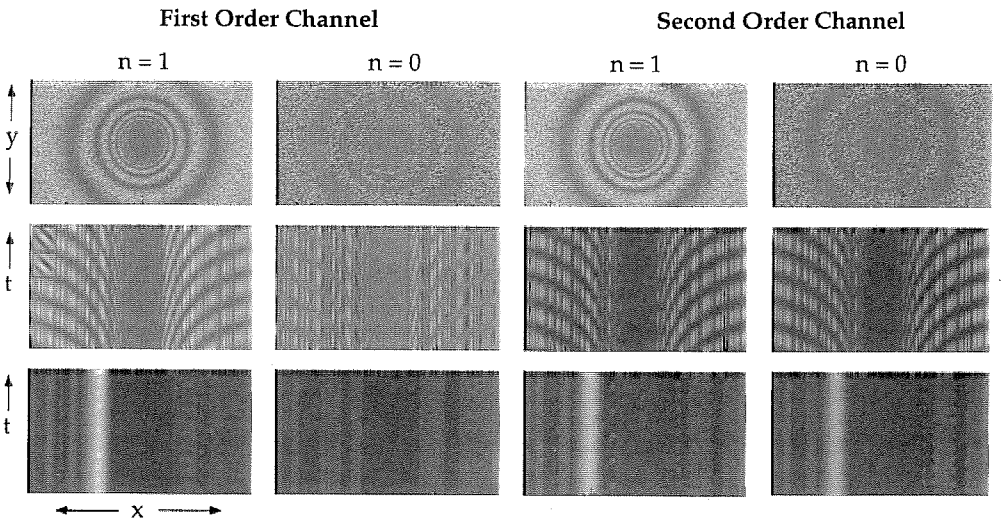


Fig. 4. Space time analysis of the stimuli. The noise carriers combined with V using $n = 1$ and $n = 0$. The middle row shows a space-time slice of the stimuli. The spatial dimension ($x$) represents a cross-section that runs through the centre of the stimulus. The left two panels of the middle row show the space-time luminance values and the right two panels show the half-rectified responses of a spatial centre-surround mechanism applied to each spatial slice. The insets in the leftmost panels show the quadrature pair Gabor signals used to extract motion energy from the space-time slice. The bottom row shows the motion energy response for each of the four stimuli. The first-order ME units (left two panels) correctly extract the direction of motion of drifting luminance peaks when $n = 1$ but not when $n = 0$. The second-order ME units (right two panels) correctly extract the direction of motion of drifting luminance peaks when $n = 1$ and when $n = 0$.

Beyond the demonstration that setting $n$ to 0 eliminates first-order ME responses to the local components of V, one can use the fact that **D** is a mean-zero signal (with no dc component), to show that the local first-order components of **S** do not lie on a plane through the origin that is consistent with the local motion of the **V**, the vection signal. Therefore, these stimuli provide a means by which to test whether the second-order channel can support vection and MAEs.

### 8.2. Radial carrier

The static concentric and noise carriers are inconsistent with the expanding motion of **V**. The radial carrier is also static as **V** expands but is not inconsistent with **V** because it is invariant to translation down the tunnel. That is, if one travelled (without pitch, yaw or roll) through a tunnel painted as in Fig. 2c no motion would be seen. Consequently modulating the radial carrier shown in Fig. 2c with the vection signal, **V**, produces motion that is consistent with an observer moving through a rigid tunnel. Using this fact, one can show that Eqs. (5) and (6) with the radial carrier produce stimuli that contain first-order motion energy consistent with **V**. Note that the actual first-order components of **V** are present in Fig. 3c and i, but not in Fig. 3f. However, all three contain first-order motion energy that is consistent with coherent motion down the tunnel. The stimulus in Fig. 3f is rather like a motion plaid comprising two components whose normal directions are not equal to the perceived direction of motion (i.e. the intersection of constraints direction). Therefore, when $n = 0$ the multiplicative combination of the Radial carrier with **V** does not produce a second-order stimulus. However, second-order ME units would respond to this stimulus in the same way that they respond to all others in Fig. 3. Furthermore, when $n = 1$ the multiplicative combination of the Radial carrier with **V** contains more first-order ME consistent with **V** than when $n = 0$.

In summary, combining the three carriers with three values of $n$ creates stimuli with different formal properties. When $n = -1$ and 1 the local first-order components of **V** are explicitly present in the signal, **S**, irrespective of carrier type. The concentric and noise carriers, however, are inconsistent with **V** and may be considered as noise. The radial carrier is consistent with **V**, and its multiplicative combination with **V** produces locally coherent (first-order) motion. When $n = 0$, the first-order components of **V** are not explicitly present in the resulting signals for any carrier type. For the concentric and noise carriers the resulting signals are standard second-order stimuli. In the case of the radial carrier the resulting signal produces locally coherent motion, in spite of the fact the local first-order components of **V** are not explicitly present. The main difference between the cases of $n = 1$ and $n = -1$ is the nature of the mean and the contrast of the stimuli.

## 9. Experiment 1

If the second-order channel conveys flow information consistent with the vection stimulus **V**, then one might

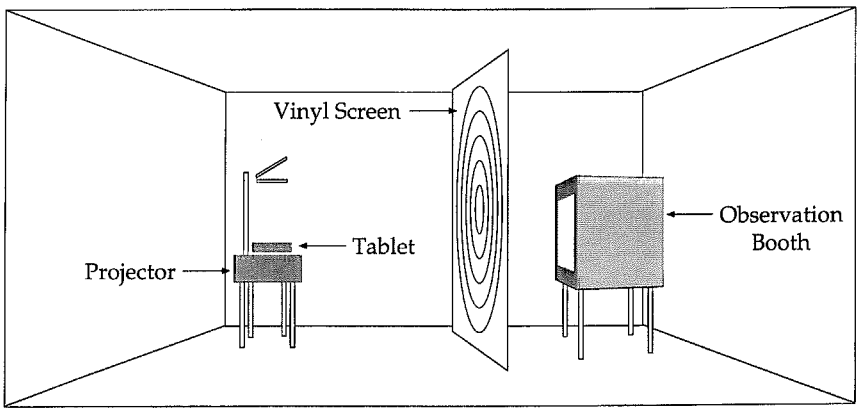


Fig. 5. Depiction of the experimental setup. Subjects sat in an observation booth (far right) from which they viewed a large vinyl screen which was parallel to the front of the observation booth. Stimuli were back projected onto the vinyl screen from a projection panel connected to a Dukane overhead projector.

expect the second-order channel to drive the vection illusion. It is known, however, that second-order motions do not always support the KDE (which is a related phenomenon) and they produce weak MAEs. It is therefore possible that second-order motion mechanisms do not support computations related to motion-in-depth. In Experiment 1 we ask if first-order and second-order motions differ in their ability to induce vection. Because existing results distinguish first-order and second-order motions both in terms of the KDE and MAE, we ask here whether our first-order and second-order motions elicit similar patterns of vection and MAE.

### 9.1. Method

#### 9.1.1. Subjects

Seven subjects participated in the experiment. Two previously participated in a similar experiment and the rest were naive to the experimental paradigm. All subjects reported normal or corrected to normal vision.

#### 9.1.2. Stimuli

There were ten different stimulus displays; the nine patterns in Fig. 3 and the control stimulus shown in Fig. 1a. The nine experimental stimuli involved the multiplicative combination of **V** with the three carriers having three different values of $n$. In one case $n$ was set close to zero at the point of psychophysical isoluminance for the carrier in question; see Appendix A for the procedure employed to determine psychophysical isoluminance. (In what follows the term 0* refers to the point of psychophysical isoluminance and 0 refers to the point of physical isoluminance.) In the other two cases $n$ was set to 1 and $-1$, thus introducing the local first-order components of **V** into the signal.

#### 9.1.3. The display

The stimuli in each of the experiments below were back-projected onto a $305 \times 230$ cm vinyl screen (CINEFLEX, rear-projection screen, Draper Shade and Screen, Spiceland, IN) using a Dukane projector and an InFocus Panel Book 550 display tablet. The tablet was controlled by a PowerMac 7100/66. Subjects viewed the screen at a distance of 120 cm from within an observation booth which was intended to enhance the realism of the motion and the induced vection ([29]). The observation booth had a rectangular window that measured $84 \times 61$ cm and there was a distance of about 60 cm from the front of the booth to the screen. Therefore the visual angle of the display inside the booth was $70 \times 54°$. Fig. 5 illustrates the essential components of the presentation system.

#### 9.1.4. Procedure

A trial consisted of a 30 s presentation of one of the ten stimulus conditions (Fig. 1a, Fig. 3a–f) followed by a 500 ms blank interval followed by a 20 s presentation of a static version of the previously moving stimulus. During the first presentation interval subjects pressed one button to indicate that they were experiencing vection and another to indicate that vection had stopped. Subjects were free to alter their responses throughout the presentation period as the illusion came and went. During the 20 s presentation of the static stimulus subjects pressed one button to indicate that they were experiencing an MAE and a second button to indicate that the MAE had dissipated. Each of the ten stimulus displays was presented six times in a random order. To enhance the realism of the display a small fixation dot was placed slightly below the centre of the screen. In the most compelling vection conditions the dot seemed to be moving along the floor of the tunnel ahead of the viewer. All testing was carried out in a darkened room.

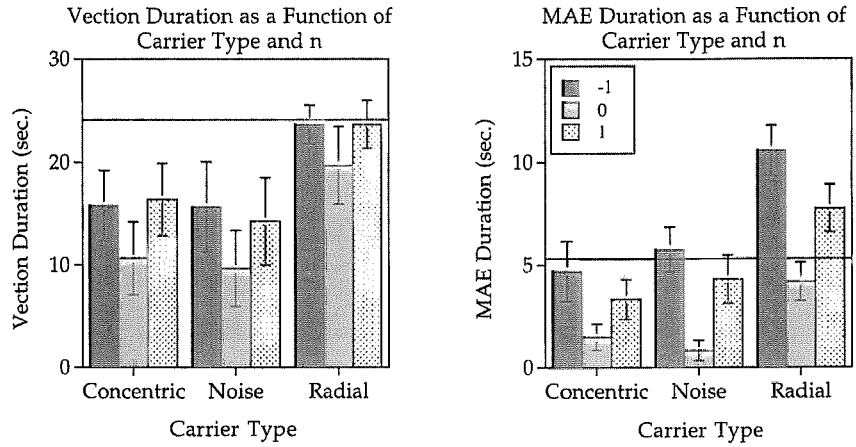


Fig. 6. Results of the vection and MAE conditions of Experiment 1. Vection durations and MAE durations are plotted as a function of carrier type (concentric, noise, radial) and $n$ ($-1$, 0* and 1). The dashed line in both panels is the mean response to the control condition.

### 9.2. Results and discussion

The average vection durations and average MAE durations were taken as the dependent measures. The control condition was not included in statistical analyses of the results. For the two dependent measures the remaining conditions were analysed as three (carriers) by three ($n$) within subjects ANOVAs. Both the vection and MAE results are summarized in Fig. 6.

In the case of the MAE, the ANOVA revealed significant main effects of carrier type ($F(2, 12) = 36.359$, $P < 0.0001$) and $n$ ($F(2, 12) = 12.551$, $P < 0.005$) and a marginally significant interaction ($F(4, 24) = 2.51$, $P < 0.07$). MAE durations yielded significant quadratic trends (as a function of $n$) in the noise and radial carriers ($F(1, 6) = 11.322$ and 24.812, respectively, both $P < 0.05$) and a marginally significant effect for the concentric carrier ($F(1, 6) = 4.192$, $P < 0.09$). Orthogonal contrasts were also used to determine if the $n = -1$ and $n = 1$ conditions differed for each carrier type. This allowed us to measure the extent to which their behaviour as a function of n is symmetric with a minima at 0*. For all three carriers the $n = -1$ conditions produce longer MAEs than did the $n = 1$ conditions. For the radial carrier the difference was significant ($F(1, 6) = 9.549$, $P < 0.01$), for the noise carrier the difference was only marginally significant ($F(1, 6) = 5.045$, $P < 0.07$) and it was not significant for the concentric carrier ($F(1, 6) = 1.607$, $P > 0.25$). As discussed above, varying n changes the mean intensity of the signal, the Michelson contrast and the mean peak to trough contrast in the signal. The relationship between MAE and $n$ (within each of the three carrier types) is most consistent with contrast defined in terms of the mean intensities at the peaks and troughs of the contrast modulation. Contrast is greatest when $n = -1$, smallest when $n = 0$* and is intermediate when $n = 1$.

In the case of vection, the ANOVA also revealed significant main effects of carrier type ($F(2, 12) = 5.914$, $P < 0.01$) and $n$ ($F(2, 12) = 19.419$, $P < 0.0005$) but no interaction. Vection durations[4] yielded significant quadratic trends in the concentric and noise carriers ($F(1, 6) = 6.414$ and 6.166, respectively, both $P < 0.05$). The quadratic trend was only marginally significant for the radial carrier ($F(1, 6) = 4.327$, $P < 0.09$). Orthogonal contrasts comparing the $n = -1$ and $n = 1$ conditions yielded no significant differences. The quadratic effects are again consistent with the conclusion that peak to trough contrast of the modulator determines performance. The fact that the $n = 1$ and $n = -1$ conditions are not significantly different suggest that vection duration is independent of overall display luminance (consistent with earlier results of [41]) and contrast.

Both vection and the MAE were significantly shorter when the local first-order components of V were absent from the stimulus. The mean vection and MAE data were highly correlated ($r = 0.90$), suggesting that the independent variables were having similar effects in both cases. Therefore, both measures depend on the total first- and second-order ME in the stimulus. Second-order mechanisms appear to make a contribution to the perception of self motion (vection responses to second-order motions were non-zero). This is consistent with the view that optic flow is computed from mechanisms that combine both first- and second-order responses ([15]) and this combined signal provides the input to units which participate in the recovery of self-motion.

The first-order/second-order distinction (noise and concentric carriers) produced larger differences in per-

[4] Anderson and Braunstein [30] found durations that ranged from 20 to 60% of 200 s presentation periods. Our results were comparable. They ranged from 32 to 80% of 30 s presentation periods.

ceptual states in the case of the MAE than in the case of vection. Consider the noise carriers from when $n = -1$ and 0*. When the first-order components of V were present the MAE lasted 5.76 s and when absent only 0.82 s. Thus MAE durations were about seven times longer when the local first-order components of V were present than when they were absent. The same comparison showed that vection durations were 1.6 times longer when the first-order components of V were present than when they were absent (15.68 and 9.66 s for $n = -1$ and $n = 0^*$ respectively). In this sense there is a divergence between the vection and MAE results.

The apparent contribution of second-order channels to vection contrast with the results of Landy et al. [19] and Dosher et al. [21]. They found a profound (virtually all or none) difference between the first- and second-order stimuli in their abilities to support the KDE. In the present experiments the first-order/second-order distinction did not lead to such a profound difference in the vection illusion. One reason for this undoubtedly has to do with task differences. Landy et al. used an objective task with a very low chance level of performance which permitted subjects' performance to reach a floor of 0% correct responses. In the present case we used subjective reports in the two tasks so subjects' responses could always be governed by internal criteria, thus permitting somewhat inflated responses. In this case we must rely tests of statistical consistency to draw conclusions about differences in mean vection and MAE durations.

On the other hand, differences between the present results and those of Landy et al. [19] may be due to differences in the stimuli used. As mentioned above, Landy et al. used displays in which the recovery of structure from motion required the integration of complex velocity signals over space and time. By contrast, the vection stimuli here involved velocity signals that were constant at each point through time (see Fig. 1). Therefore, the relative simplicity of the vection signal may have made the recovery of motion-in-depth easier than in the Landy et al. study. This is consistent with Prazdny [22] who reports that simple 3D structures could be recovered from second-order motions.

## 10. Experiment 2

Smith and Ledgeway [42] have argued that static carriers, such as those used in Experiment 1, may be poor choices for the construction of second-order motion stimuli. For the noise carrier in particular, they argue that the drifting contrast modulation may be contaminated by local first-order motions arising from 'stochastic local biases in the noise' (p. 45). Smith and Ledgeway point out that as the check size of the pixels increases (see Fig. 7) so does first-order contamination.

To demonstrate this point, the motion analysis described in Fig. 4 was repeated for contrast modulated noise ($n = 0$) in which the noise 'check size' varied from one to 128 pixels. The motion stimulus was a leftward moving sine wave grating with a wavelength of 16 pixels. An ME mechanism tuned this spatiotemporal signal was applied both to the raw image intensities (first-order channel) and to rectified responses of a small differential operator as described in Fig. 4 (second-order channel). An ME unit tuned to the opposite direction of motion was also applied to the same stimuli. Left and right ME responses were summed over 92 cycles of the contrast modulation and their difference was passed through a compressive nonlinearity; i.e. log (left-right). The filled circles in Fig. 8 plot the first-order ME responses as a function of noise check size. It is

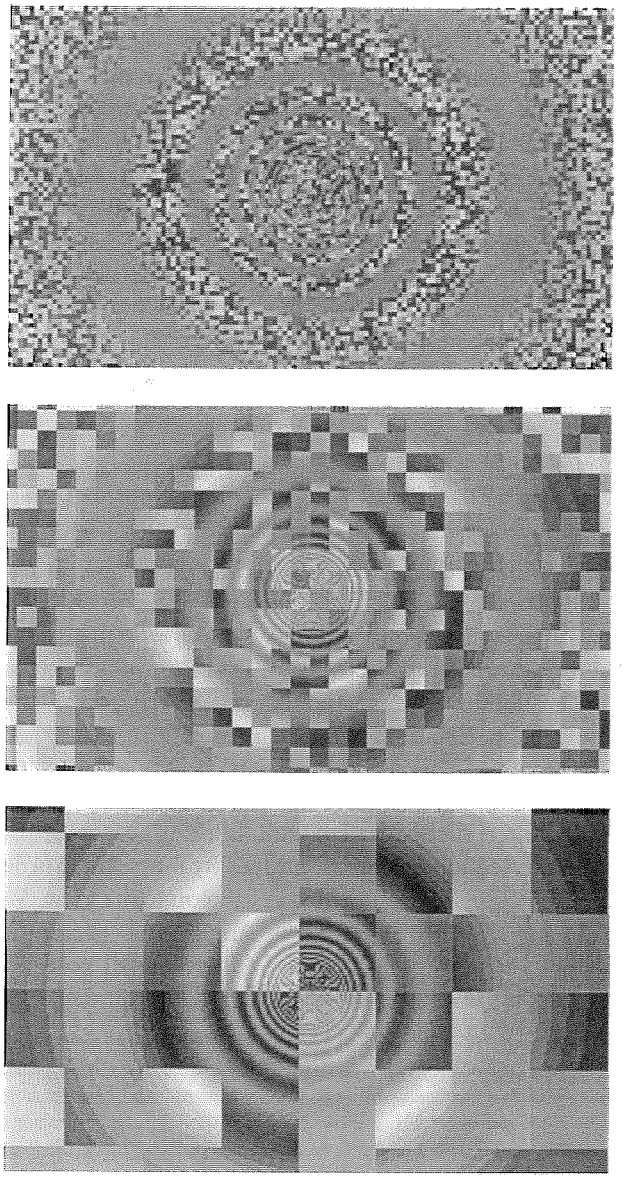

Fig. 7. Examples of the stimuli used in Experiment 2.

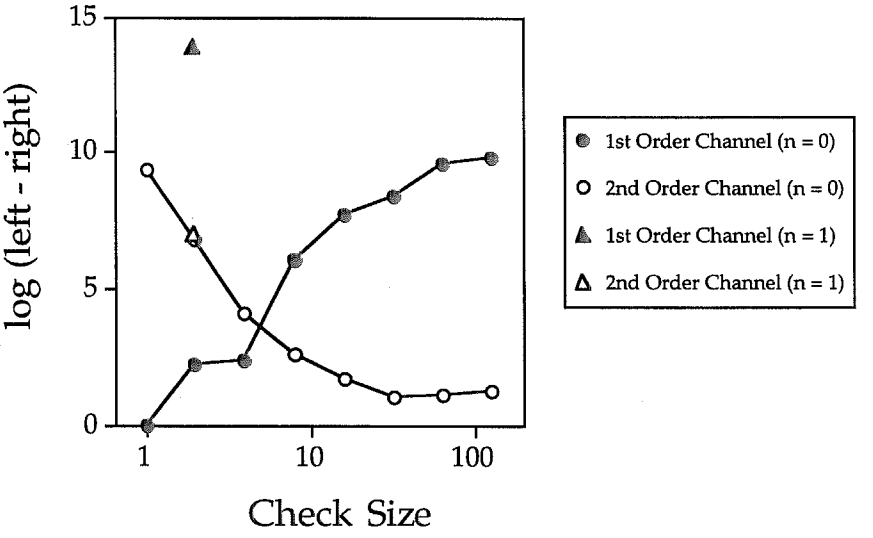


Fig. 8. Motion energy analysis of the stimuli used in Experiment 2. See text for details of the analysis. First-order ME increases as check size increases whereas second-order ME decreases as check size increases.

clear that local first-order motion energy increases as check size increases. As well, note that there are small first-order ME responses for the check size (two square pixels) used in Experiment 1, consistent with the arguments of Smith and Ledgeway [42]. The unfilled circles plot the second-order ME responses, which decrease as a function of check size.[5] Although the particular second-order channel described here is somewhat arbitrary, it embodies the essential elements of second-order channels described in the literature and allows a qualitative examination of the change in first- and second-order ME responses with check size.

The filled and open triangles show the same ME responses when applied to the stimuli of Experiment 1; check size $= 2 \times 2$ pixels and $n = 1$. The second-order ME responses are essentially the same for $n = 0$ and $n = 1$ (open circle and open triangle respectively). The first-order ME responses for $n = 0$ and $n = 1$ (filled circle and filled triangle respectively) are substantially different and presumably explains the reduced MAEs and vection durations in Experiment 1 when $n = 0$*.

In terms of this analysis it may be argued that the second-order channel does not necessarily support vection. Rather, first-order contamination may explain the moderate vection responses induced by our second-order stimuli. A second argument takes the opposite view. We made no effort to equate our stimuli for 'perceptual salience' or perceptual contrast. Therefore, it could be argued that first- and second-order stimuli induce vection equally well but our first-order stimuli have higher perceptual contrast than our second-order stimuli and this account for the observed differences. We address these arguments in turn.

Smith and Ledgeway [42] have argued that dynamic carriers—in which binary noise checks are changed randomly on each frame—provide the best method of eliminating residual first-order structure from a motion sequence. Dynamic carriers would offer an alternative that arguably contains less first-order structure than our static carriers but in our view they would introduce undesirable complications. Smith and Ledgeway observed that detection thresholds for contrast modulations of dynamic carriers are higher than contrast modulations of static carriers. The implication is that residual first-order structure in the static carriers reduces thresholds. There are two reasons to question this conclusion. First, a static noise carrier has higher perceptual contrast than one flickered at a high rate (as in Smith and Ledgeway's study). Reducing perceptual contrast in this way might increase the contrast modulation required to detect the modulator (just as found by Smith and Ledgeway). One can also argue that dynamic noise produces larger amounts of spatiotemporal noise in second-order channels relative to static carriers, which decreases the detectability of the drifting contrast modulator. For these reasons, if vection responses were found to be further attenuated when dynamic carriers are employed one could not necessarily conclude that second-order motions do not induce vection. In view of these questions about the conclusions one can draw from dynamic versus static carriers we feel that the dynamic carriers would be an interesting third carrier type, but not a critical alternative. Furthermore, the significantly reduced MAEs found when $n = 0$* in Experiment 1 are consistent with the elimination of first-order ME.

[5] It may not be obvious that the response of the second-order channel should decrease with check size. It must be borne in mind that the second-order ME unit is applied to the rectified responses of a first layer differential operator. As check size increases there are larger and larger regions with no intensity variation and consequently, no responses from the first layer differential operator.

The second issue is that first- and second-order stimuli may differ in perceptual 'salience'. The question then becomes: how are first- and second-order stimuli to be equated? One approach would be to set the luminance and contrast modulations to the same multiple of threshold. This assumes that luminance and contrast modulations scale in the same way, but there is no reason to believe that this is the case. An electric current at ten times threshold is considerably more 'salient' than a white light at ten times threshold ([43]; see [44] for a related discussion). The same may be true for luminance-and contrast-modulations. Furthermore, it is known that the perceptual contrast of gratings generally cannot be equated by setting them to equal multiples above detection threshold [45]. Cross-modal matching would be a good way to equate the 'salience'of two stimuli but is difficult to apply to the salience of luminance modulations versus contrast modulations. In our attempts to do this subjects found it difficult to attach meaning to the idea of more or less salient motion, independent of the contrast in the carrier.

To deal effectively with both concerns, in Experiment 2 we employed the Smith and Ledgeway check size manipulation to determine how MAEs and vection are affected by variations in the strength of the local first-order components of the V. This manipulation keeps all measures of physical contrast constant and provides a reasonable method of equating the salience of the stimuli while varying first-order ME content. First-order ME units would be more strongly stimulated with larger check sizes so MAEs should increase with check size. The main question is whether vection durations would follow the same pattern. If the modest vection durations found for the second-order stimuli in Experiment 1 arise from residual first-order contamination then vection durations should also increase with check size. On the other hand, if first and second-order motions combine to elicit vection then, from the ME analysis in Fig. 8 we might expect a quadratic dependence of vection on check sizes or possibly no effect of check size, depending on the relative contributions of the first and second-order channels.

### 10.1. Method

#### 10.1.1. Subjects

Six subjects participated in Experiment 2. Three of these had also participated in Experiment 1. All subjects reported normal, or corrected to normal vision.

#### 10.1.2. Stimuli

The experimental stimuli consisted of the multiplicative combination ($\mu = 1.33$, $\alpha = 0.6$) of V with static noise carriers having various check sizes. Eight check sizes were employed (check width $= 2^m$ pixels, for $m$ in [0, 7]) and a control stimulus that consisted of the modulator alone. See Fig. 7 for example stimuli.

#### 10.1.3. Procedure

The procedure was exactly as in Experiment 1 except that equivalent luminance was not calculated for the eight different check sizes. There are two reasons for this. First, Smith and Ledgeway [42] showed that global distortion products had little effect on the pattern of results obtained when check size was manipulated. This means that had equivalent luminance not been computed in Experiment 1 the results would probably not have changed. Second, even though non linearities in the visual system may result in responses from first-order ME units, the magnitude to first-order ME responses will vary systematically with check size and will permit a comparison of the psychometric functions for vection and MAE durations. Each of the ten stimuli was presented five times in a random order.

### 10.2. Results and discussion

Fig. 9 plots the mean MAE and vection durations as a function of check size. The horizontal line indicates the MAE and vection responses to the control stimulus. A one factor, within subjects ANOVA applied to the the MAE data (excluding the control condition) revealed a significant effect of check size ($F(7, 35) = 10.861$, $P < 0.0001$). A Neuman–Keuls, *post-hoc* test showed that check sizes of 1, 2 and 4 pixels were significantly different from the control stimulus at the 0.05 level. The MAEs are exactly what would be predicted from the results of Smith and Ledgeway [42]. With very small check sizes most first-order ME is

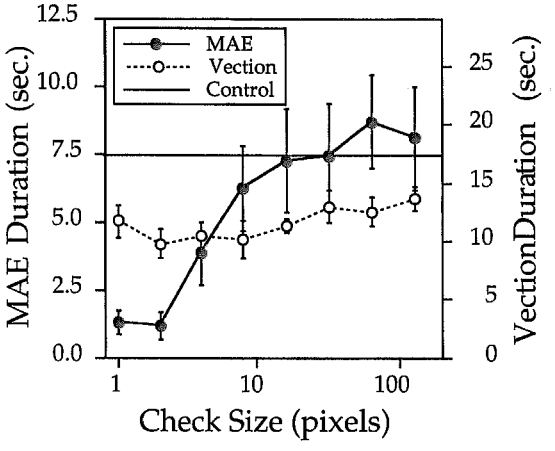


Fig. 9. The results of Experiment 2. The left and right axes relate to MAE and vection durations, respectively. The axes have been scaled to match performance in the control conditions (solid horizontal bar) of the two tasks. MAE durations (filled circles) increase with check size and asymptote at the level of the control stimulus. Vection durations (unfilled circles) are always significantly below the level of the control stimulus and are unaffected by check size.

eliminated from the stimulus and the standard reduction of MAE is found. As check size increases more and more first-order ME becomes available and the MAE approaches the magnitude of the control stimulus.

A one factor, within subjects ANOVA applied to the the vection data (excluding the control condition) showed that vection duration does not change significantly with check size ($F(7, 35) = 1.526$, $P > 0.19$). Furthermore, the Neuman–Keuls test indicated that no two individual means were significantly different from each other. On the other hand, vection durations for all check sizes were significantly different from the control condition at the 0.05 level. The results show a very clear dissociation between the MAE and vection durations. Therefore, a principle conclusion from Experiment 2, is that modest vection illusion induced by the second-order stimuli in Experiment 1 is not the result of first-order contamination in our second-order stimuli.

## 11. General discussion

The experiments were motivated by observations that first- and second-order motions differ in their ability to induce MAEs and, under certain conditions, the KDE. This suggests that despite similarities in their computational structure, first- and second-order motion mechanisms might subserve different functions. To address this question we examined a vection stimulus representing a linear path through a circular tunnel. The vection stimulus V was combined multiplicatively with a number of different carriers. The resulting signals differed in the amount of first- order ME (associated with V) they contained.

Experiment 1 showed a first-order 'advantage' for both vection and MAE. The vection results are generally consistent with idea that first- and second-order motion channels combine in the computation of optic flow [15] and that removing one reduces the vection experience. (This result is consistent with a recent report by Ashida et al. [46] that first-order motions induce greater postural adjustments than do second-order motions.) Experiment 2 showed vection to be independent of the amount of local first-order ME and a dissociation with the MAE results. The MAE results were what would be expected (based on past observations that MAEs are stronger when the first-order components are present). The vection results suggest that a rather abstract representation of optic flow is sufficient to drive the self motion response.

There may appear to be an inconsistency in the results of the two experiments: the presence of the first-order components of V had a significant effect on vection durations in Experiment 1 but not in Experiment 2. This difference is easily explained in terms of the ME analysis presented in Fig. 8. In Experiment 1 there are strong second-order and weak first-order responses when $n = 0$ and strong first- and second-order responses when $n = 1$. This accounts for the significant effect of $n$. By contrast in Experiment 2 first- and second-order ME responses trade-off as a function of check size such that second-order responses increase as first-order responses decrease. If first- and second-order responses combine to elicit vection then, depending on the nature of the combination rule, an independence of check size is one of the results that could be expected. Given that in both Experiments 1 and 2 vection was induced when first-order ME was drastically attenuated, if not eliminated, we may conclude that second-order motion signals contribute to the vection illusion.

In both Experiments 1 and 2 MAEs were generally less affected by the presence of a static, inconsistent carrier (noise and concentric carriers) than were vection durations. In Experiment 2 MAE durations increased with check size and asymptoted at the same level as the control stimulus. Similarly, in Experiment 1, when $n = 1$ and $-1$ the noise and concentric carriers elicited MAE similar to that of the control stimulus (with the possible exception of the concentric carrier when $n = 1$). In other words, the MAE is generally unaffected by the presence of a static, inconsistent carrier when the first-order components of V are present. In contrast, for all check sizes in Experiment 2 vection durations were shorter than in the control condition. As well, in Experiment 1, when $n = 1$ and $-1$ vection durations for the concentric and noise carriers were shorter than for the control stimuli. The differential effects of the static, inconsistent carriers in the two tasks might indicate two levels of motion analysis.

The MAE may arise in conventional ME units typically associated with V1 [47,48] resulting from either fatigue [49] or recalibration [50–52]. Vection may arise from a more abstract representation of optic flow. Area MT is often described as a site of integration of first and second-order motion signals [15]. Duffy and Wurtz [39,40] have reported that cells in area MSTd respond to optic flow stimuli. It may be that first and second-order motion channels converge on area MT where these signals are integrated and conveyed to MSTd. This would lead to the speculation that MSTd cells, including those that respond to optic flow, may be driven by both first and second-order motion signals.

The idea that aftereffects are associated with low- rather than high-level representations is consistent with results in the colour literature. Thompson and Latchford [53], for example, showed that so-called colour contingent aftereffects (i.e. McCollough effects) are governed by the predominant wavelength reflected from a surface not by the perceived colour of the surface. Our results may reflect something similar. Representations of motion that combine first and second-order

information may be considered relatively high level or abstract. Aftereffects may then reflect the adaptation of low-level motion mechanisms rather than this higher level construction.

Although a simple account of the present data can be given in terms of first- and second-order ME units, motion transparency may provide an alternative theoretical vocabulary with which to describe the results. In Experiment 2, for example, all stimuli consisted of grey rings moving over checks of various sizes which may be described as a combination of multiplicative and additive transparency, irrespective of check size [26,27,14]. The density of the occluding surface (which itself reflects light) changes from point to point. All cases may then induce the percept of travelling though 'smoke rings' towards an a distant surface. Given that the transparency relations don't change with check size this may explain why vection durations don't change significantly either. In other words, sensitivity to transparency relations permit the segregation of the motion signal from the static checks and this 'interpreted' signal then drives vection. Even though transparency relations may permit the segregation of the motion signal from the static carrier the presence of the carrier weakens the sense of self motion relative to the control stimulus. From the motion energy point of view the static carrier is inconsistent with the motion signal (whether conveyed by first or second-order channels) and has a masking effect. From the transparency point of view the checks may be uniformly disruptive because they do not change size over time, as they should if they were at some moderate distance from viewer, thus conflicting with the motion signal. Although transparency provides a different way of looking at the results of Experiment 2, it is not clear how it applies to the results of Experiment 1. In any case ME channels and transparency are related analyses [27,14]. The present experiments were structured by questions arising from the distinction between first- and second-order ME mechanisms. Whether or not transparency computations play a role in the present results, the fact remains that second-order motion contributes to vection.

## Acknowledgements

This research was supported by NSERC and FCAR Research Grants to Rick Gurnsey and David Fleet, an Alfred P. Sloan Research Fellowship to David Fleet and an FCAR graduate scholarship to Cindy Potechin. We thank Michael von Grünau, Frédéric Poirier and Eric Gascon for their comments on the research described in this report, Barrie Frost for his input early in the development of this project, and Peter April for excellent programming support.

## Appendix A. Computing 'equivalent luminance' for each subject

All carrier signals discussed in the text were mean zero so that when $n = 0$ the mean luminance should be the same ($\mu$) at all points in the stimulus. Under these conditions the Fourier components of V are not physically present in the stimulus. If, however, there are small nonlinearities in the transduction process, for example, then the transduced signal may not be 'isoluminant'. In this case some of the motion energy of V will be introduced into stimuli as an artifact. Consequently if MAE and vection results were found to be equivalent for first- and second-order motions then one might not be able to attribute this similarity to equipotent effects of first- and second-order channels; similar issues arise when 'isoluminant' colours are studied [54]. Therefore, before proceeding with the vection and MAE experiments, it was decided to modify the stimuli slightly, in an attempt to cancel very early nonlinearities in the visual system that might introduce motion energy that is consistent with the vection signal. Rather than using $n = 0$ to produce 'isoluminant' stimuli we adjusted $n$ slightly for each subject and for each carrier type to establish the point of psychophysical isoluminance using the method described by Brown [55].[6]

To establish psychophysical isoluminance two low frequency (0.25 cpd) counter phase vertical sine wave gratings were interleaved with two counterphase gratings defined by contrast modulations which were displaced by a quarter cycle from their sine wave counterparts. Three carriers for the contrast modulations were used to create stimuli that corresponded as closely as possible to the modulator/carrier relationships of the stimuli used in the experiment (Fig. 3 b, d and f). One carrier was vertical with a spatial frequency three times that of the vertical modulator. This corresponds to the concentric carrier which was locally parallel to the modulator. Another carrier was random noise, like that described in Fig. 2c and Fig. 3d. The last carrier was horizontal having a frequency three times that of the vertical modulator, analogous to the local orthogonality of the carrier and modulator seen in Fig. 3f. If in Fig. 10a the high contrast regions of the contrast modulations had a higher perceptual luminance than the low contrast regions then motion would be seen to the left and in the obverse case motion would be seen to the right. At the point of psychophysical isoluminance (equivalent luminance) the motion should be ambiguous.

Subjects were presented with 15 s samples of the stimuli and asked to press predetermined keys on the

[6] Ideally we would like to apply the inverse nonlinearity to the stimulus. Changing $n$ is a crude, but effective approximation to the inverse of the nonlinearity.

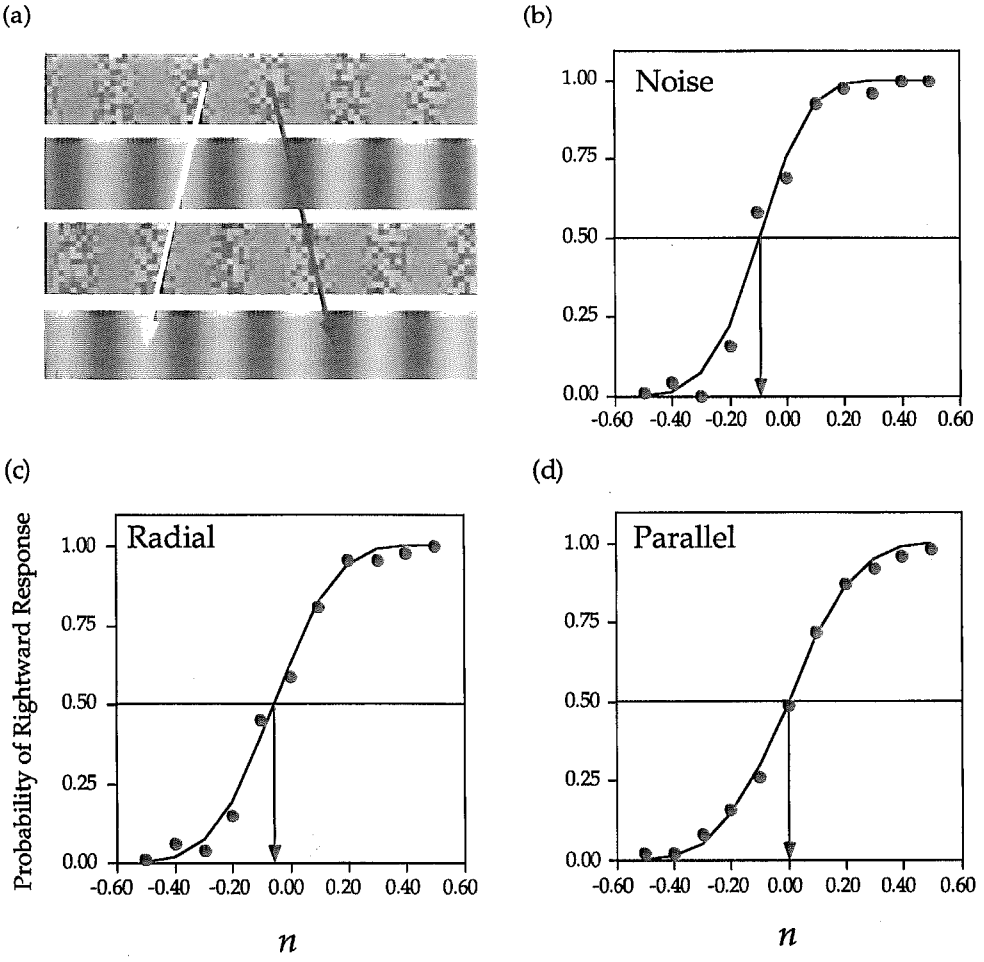


Fig. 10. The method of establishing the point of perceptual equiluminance between high and low contrast regions of stimuli. (a) Two counterphase sine waves were interleaved with two counterphase contrast modulated carriers; the contrast modulators were a quarter cycle out of phase with sine wave on the previous frame. The low contrast region of the contrast modulated carrier was fixed in intensity and the high contrast region varied with n from Eq. (4). When $n$ was much less than zero, the high contrast regions of the modulated carrier had lower mean intensity than the low contrast (grey) regions and would match the troughs of the sine wave presented on the next frame. When $n$ was much greater than zero, the high contrast regions of the modulated carrier had high mean intensity than the low contrast regions and would match the peak of the sine wave presented on the next frame. At the point of perceptual equiluminance, motion was ambiguous. During 15 s presentations of the sequence shown in (a), subjects pressed predetermined keys on the keyboard to indicate whether they were seeing motion to the left or to the right. The point at which both responses had a 50% chance of occurring was taken to be the point of perceptual equiluminance. Panels b–d show the average results for the six subjects along with the best fitting Weibull function, for the three carrier types.

keyboard to indicate whether the perceived direction of motion was rightward or leftward [56,10]. Subjects were informed that some stimuli would induce highly bistable percepts, altering frequently from rightward to leftward motion, and that others would be more stable, yielding a single interpretation throughout the 15 s presentation. The method of constant stimuli was used with $n$ ranging from $-0.5$ to 0.5 in steps of 0.1. For each carrier type the stimuli were presented in a random order with two replications of each value of $n$. For each value of $n$ the average ratio of rightward to rightward + leftward ($R/(R+L)$) responses was computed. The point at which the linear interpolation of the resulting function crossed 0.5 was taken as the point of equivalent luminance. These calculations agree well with the 0.5 points on the best fitting Weibull functions (least squares minimization technique). The average discrepancies between the two methods, expressed as a proportion of the range of $n$ (i.e. 2) were 0.009, 0.013 and 0.015 for the parallel, orthogonal and noise carriers respectively.

Fig. 10b–c shows the average results of six subjects along with the best fitting Weibull function. The point of equivalent luminance was typically less than the point of physical isoluminance for the noise and orthogonal carriers (consistent with the results of Brown [55]) and very close to physical isoluminance for the parallel carrier. Thus, in the text, for those stimuli in which we wish to avoid the presence of motion energy consistent with the vection signal **V**, we use this measure of $n$, denoted 0*, rather than $n = 0$.

## References


[1] Adelson EH, Bergen JR. Spatiotemporal energy models for the perception of motion. J Opt Soc Am A 1985;2:284–99.

[2] Watson AB, Ahumada AJ Jr. Visual-Motion Sensing. J Optical Soc Am 1985;A2:322–41.

[3] Fleet, DJ. Measurement of image velocity. Kluwer Academic Publishers, MA: Norwell, 1992.

[4] Simoncelli EP, Heeger DJ. A model of neural responses in visual area MT. Vis Res 1988;38:743–761.

[5] Cavanagh P, Mather G. Motion: the long and short of it. Spatial Vision 1989;4:103–29.

[6] Chubb C, Sperling G. Drift-balanced random stimuli: a general basis for studying non-Fourier motion perception. J Opt Soc Am 1988;A5:1986–2007.

[7] Ledgeway T, Smith A. The duration of the motion aftereffect following adaptation to first-order and second-order motion. Perception 1994;23:1211–9.

[8] Turano K, Pantle A. On the mechanism that encodes the movement of contrast variations: Velocity discrimination. Vision Res 1989;29:207–21.

[9] Wilson HR, Mast R. Illusory motion of texture boundaries. Vision Res 1993;33:1437–46.

[10] Gurnsey R, von Grünau M. Illusory contour-motion arising from translating terminators. Vision Res 1997;37:1007–24.

[11] Zanker, JM. How motion detectors respond to some illusory contours. In: Blum B, editor. Channels in the Visual Nervous System: Neurophysiology, Psychophysics and Models. London: Freund, 1991.

[12] Zanker JM. Theta motion: a paradoxical stimulus to explore higher order motion extraction. Vision Res 1993;33:553–69.

[13] Boulton JC, Baker CL Jr. Dependence on stimulus onset asychony in apparent motion: evidence for two mechanisms. Vision Res 1993;33:2013–9.

[14] Fleet DJ, Langley K. Computational analysis of non-fourier motion. Vision Res 1994;34:3057–79.

[15] Wilson HR, Ferrera VP, Yo C. Psychophysically motivated model for two-dimensional motion perception. Vis Neurosci 1992;9:79–97.

[16] Ledgeway T, Smith A. The perceived speed of second order motion and its dependence on stimulus contrast. Vision Res 1995;35:1421–34.

[17] Mather G. First-order and second-order visual processes in the perception of motion and tilt. Vision Res 1991;31:161–7.

[18] Nashida S, Ashida H, Sato T. Complete interocular transfer of motion aftereffect with flickering test. Vision Res 1994;34:2707–16.

[19] Landy MS, Dosher BA, Sperling G, Perkins ME. The kinetic depth effect and optic flow-II: first- and second-order motion. Vision Res 1991;31:859–76.

[20] Sperling G, Dosher BA, Landy MS. How to study the kinetic depth effect experimentally. J Exp Psychol: Human Perception Performance 1990;15:826–40.

[21] Dosher BA, Landy MS, Sperling G. Kinetic depth effect and optic flow- I: 3D shape from Fourier motion. Vision Res 1989;29:1789–813.

[22] Prazdny K. Three-dimensional structure from long range apparent motion. Perception 1986;15:619–25.

[23] Sperling G, Dosher BA. Depth from motion. In: Papathomas T, Chubb C, Gorea A, Kowler, E, editors. Early Vision and Beyond. Cambridge: The MIT Press, 1995: 133–143.

[24] Livingstone M, Hubel D. Segregation of form, color, movement, and depth: anatomy, physiology, and perception. Science 1988;240:740–9.

[25] Wuerger SM, Landy MS. Role of chromatic and luminance contrast in inferring structure from motion. J Opt Soc Am 1993;A10:1363–72.

[26] Kersten, D. Transparency and the cooperative computation of scene attributes. In: Landy MS, Movshon AJ, editors. Computational Models of Early Visual Processing. Cambridge, MA: MIT Press, 1991: 209–228.

[27] Mulligan JB. Nonlinear combination rules and the perception of visual motion transparency. Vision Res 1993;33:2021–30.

[28] Fleet DJ, Langley K. NonFourier channels in stereopsis and motion. ECVP94, Eindhoven, September (in Perception 1994; 23: supplement page 35.)

[29] Telford L, Frost BJ. Factors affecting the onset and magnitude of linear vection. Percept Psychophys 1993;53:682–92.

[30] Anderson GJ, Braunstein ML. Induced self-motion in central vision. J Exp Psychol: Human Perception and Performance 1985;11:122–32.

[31] Howard IP, Heckmann T. Circular vection as a function of the relative sizes, distances, and positions of two competing visual displays. Perception 1989;18:657–65.

[32] von der Heydt R, Peterhans E, Baumgartner G. Illusory contours and cortical neuron responses. Science 1984;224:1260–2.

[33] Grosof DH, Shapley RM, Hawken MJ. Macaque V1 neurons can signal 'illusory' contours. Nature 1993;365:550–2.

[34] Zhou YX, Baker CL Jr. A processing stream in mammalian visual cortex neurons for non-Fourier responses. Science 1993;261:98–101.

[35] Zhou YX, Baker CL Jr. Envelope-responsive neurons in areas 17 and 18 of cat. J Neurophysiol 1994;72:2134–50.

[36] Albright TD. Form-Cue invariant motion processing in primate visual cortex. Science 1992;255:1141–3.

[37] O'Keefe, LP, Movshon, JA. Neuronal responses to first- and second-order motion in the superior temporal sulcus of the alert macaque. Investigative Ophthalmology and Visual Science 1997 38(4), ARVO Abstract Supplement.

[38] Movshon JA, Adelson EH, Gizzi MS, Newsome WT. The analysis of moving patterns. In: Chagas C, Gattass R, Gross C, editors. Pattern Recognition Mechanisms. Berlin: Springer, 1986: 117–151.

[39] Duffy CJ, Wurtz RH. Sensitivity of MST neurons to optic flow stimuli. I. a continuum of response selectivity to large-field stimuli. J Neurophysiol 1991;65:1329–45.

[40] Duffy CJ, Wurtz RH. Sensitivity of MST neurons to optic flow stimuli. II. mechanisms of response selectivity revealed by small-field stimuli. J Neurophysiol 1991;65:1346–59.

[41] Leibowitz HW, Rodemer CS, Dichgans J. The independence of dynamic spatial orientation from luminance and refractive error. Percept Psychophys 1979;25:75–9.

[42] Smith AT, Ledgeway T. Separate detection of moving luminance and contrast modulations: fact or artifact? Vision Res 1997;37:45–62.

[43] Stevens, SS. The psychophysics of sensory function. In: Rosenblith WA, editor. Sensory Communication. Cambridge MA: MIT Press, 1961: 1–33.

[44] Fechner G. The Elements of Psychophysics. [Alder HE, Trans.] New York: Holt, Rinehart and Winston, 1960.

[45] Cannon M. Perceived contrast in the fovea and periphery. J Opt Soc Am 1985;A2:1760–8.

[46] Ashida, H, Robin, N, Kaneko, H, Verstraten, F, Ojima, S. Second-order motion has little effect on human postural control. Invest Ophthalmol Visual Sci 1997; 38(4), ARVO abstract supplement.

[47] DeAngelis GC, Ohzawa I, Freeman RD. Spatiotemporal organization of simple-cell receptive fields in the cat's striate cortex. I. General characteristics and postnatal development. J Neurophysiol 1993;69:1091–117.

[48] DeAngelis GC, Ohzawa I, Freeman RD. Spatiotemporal organization of simple-cell receptive fields in the cat's striate cortex. II. Linearity of temporal and spatial summation. J Neurophysiol 1993;69:1118–35.

[49] Barlow HB, Hill RM. Selective sensitivity to direction of motion in ganglion cells of the rabbit's retina. Science 1963;139:412–4.
[50] Helson H. Adaptation-level as a basis for a quantitative theory of frames of reference. Psychol Rev 1948;55:297–313.
[51] Andrews DP. Error-correcting perceptual mechanisms. Q J Exp Psychol 1964;16:104–15.
[52] Ullman S, Schechtman G. Adaptation and Gain Normalization. Proc R Soc London 1982;B216:299–313.
[53] Thompson P, Latchford G. Colour-contingent after-effects are really wavelength-contingent. Nature 1986;320:525–6.
[54] Cavanagh P, Anstis S. The contribution of color to motion in normal and color-deficient observers. Vision Res 1991;31:2109–48.
[55] Brown, RO. Luminance non-linearities and second order stimuli. Invest Ophthalmol Visual Sci 1995; 36(4), ARVO abstract supplement.
[56] von Grünau MW, Dubé S. Ambiguous plaids: switching between coherence and transparency. Spat Vis 1993:199–211.